

## BERYLLIUM ABUNDANCES IN THE LITHIUM-DEFICIENT HYADES F STARS

ANN MERCHANT BOESGAARD<sup>1</sup>

Institute for Astronomy, University of Hawaii

AND

KENT G. BUDGE<sup>1</sup>

Palomar Observatory, California Institute of Technology

*Received 1988 July 6; accepted 1988 August 29*

## ABSTRACT

The Be abundance of a main-sequence star is an indication of the depth and extent of convective mixing, since beryllium is destroyed at moderately low temperatures:  $\sim 3.5 \times 10^6$  K. This is to be compared with a temperature of  $\sim 2.5 \times 10^6$  K for Li. We have obtained spectra of the Be II doublet at 3130.4 and 3131.1 Å in eight Hyades F dwarfs, including stars in the Hyades Li gap found by Boesgaard and Trippico. Observations were made at CFHT on the nights of 1986 October 11 and December 11 and 12 at the coudé focus with the ultraviolet optical train and a Texas Instruments CCD as the detector. The dispersion was  $0.05 \text{ Å pixel}^{-1}$  and the signal-to-noise ratio was typically  $\sim 100$ . Abundances were determined in the standard way, but in addition a “differential spectroscopy” procedure was used. This involved comparing the Hyades stars with a standard star via a least-squares algorithm to give the best fit between the object and standard spectra in the region immediately around the Be doublet. This procedure was adapted to rapidly rotating stars by convolving the standard spectrum with a rotation profile of the correct width. A synthesis of the spectrum was done also with 20 spectral lines in the region of the Be blend. There is virtually no change in the Be content in these stars across the temperature region where there is a large deficiency in Li. The Be/H values are  $\sim 10^{-11}$ , near the solar value of  $1.4 \times 10^{-11}$ .

*Subject headings:* clusters: open — stars: abundances

## I. INTRODUCTION

The abundances of both Li and Be in main-sequence stars are indicators of the depth and extent of convective mixing, since Li is destroyed at  $\sim 2.5 \times 10^6$  K and Be at  $\sim 3.5 \times 10^6$  K. Due to this temperature (and thus depth) difference for the destruction of Li versus Be, Be-deficient stars would be expected to be Li-deficient, which indeed they are (Boesgaard and Lavery 1986), but Li-deficient stars would not necessarily be Be-deficient.

The Hyades F dwarfs show a surprising Li-temperature profile first discovered by Boesgaard and Tripicco (1986) and extended by Boesgaard and Budge (1988). Stars hotter than  $\sim 6800$  K have  $\log N(\text{Li}) \sim 3.0$  [where  $\log N(\text{H}) = 12.00$ ]. This is followed by a sharp drop in Li toward stars with limits of  $\log N(\text{Li}) \lesssim 1.3$  at 6650 K and then a slower rise back up to  $\sim 3.0$  near 6300 K. In order to map the extent of the convective mixing, we have made observations of the resonance lines of Be II at  $\lambda\lambda 3130$  and  $3131$  through the Li dip in the Hyades. Preliminary results from these observations were reported by Budge, Boesgaard, and Varsik (1988). Photographic observations of Be II in six Hyades F dwarfs were made by Boesgaard, Heacox, and Conti (1977) who found a mean Be/H =  $1.0 \times 10^{-11}$ . The ratio of Li/Be is of interest as a probe of convection, and where neither element is deficient, as an indicator of the light-element formation processes. Be is formed exclusively by cosmic-ray spallation while Li is formed in the big bang and by spallation. The Be abundance gives a measure of cosmic-ray activity during the lifetime of the Galaxy.

## II. OBSERVATIONS

We have obtained spectra of eight F main-sequence stars near and in the Hyades Li gap. Observations were made at CFHT on the nights of 1986 October 9 and 10 and December 10 and 11, UT. Spectra were obtained at the coudé focus using the ultraviolet optical train and a TI  $500 \times 500$  CCD as the detector. For the October data the 830 lines per mm grating gave a dispersion of  $0.033 \text{ Å pixel}^{-1}$  and the signal-to-noise ratio (S/N) was typically  $\sim 70$ . To improve the efficiency of the system, the 600 lines per mm grating was used in the December run. The dispersion was  $0.046 \text{ Å pixel}^{-1}$  and S/N typically 100–130. Although progress has been made in increasing the blue sensitivity of CCD detectors, exposures of 30–100 minutes were required to obtain those signal-to-noise ratios. Some field stars were observed for comparison with the Hyades stars. The stars observed, some of their known properties, and the S/N values are given in Table 1.

## III. REDUCTION OF DATA

The spectra have been flat-fielded and dark-subtracted; the cosmic-ray signatures have been removed by an interpolation process from adjoining pixels. The spectral region near the Be doublet is heavily line-blanketed, making it difficult to determine the true continuum level. This line blanketing also results in numerous blends, which are further accentuated by the rapid rotation of many stars of interest in this temperature range.

We have used three approaches to find the Be abundances in these stars. First, the direct way of fitting a continuum through the nearby “windows,” measuring the strength of the relatively unblended Be II line at  $\lambda 3131$ , and finding the abundance from the predictions of the equivalent widths from a grid of model

<sup>1</sup> Visiting Astronomer at the Canada-France-Hawaii Telescope, operated by the National Research Council of Canada, the Centre National de la Recherche Scientifique of France, and the University of Hawaii.

TABLE 1  
STARS OBSERVED

VB/Name	HD	1986 date	S/N	$T$	$v \sin i$
14 .....	26462	Dec 11	110	7040	6
37 .....	27561	Dec 11	130	6815	12
13 .....	26345	Dec 11	120	6725	18
124 .....	30869	Dec 12	100	6630	25
128 .....	31845	Dec 11	105	6560	25
78 .....	28407	Oct 11	70	6510	20
86 .....	28608	Dec 12	100	6485	20
81 .....	28483	Dec 12	100	6470	18
$\alpha$ CMi .....	61421	Dec 12	330	6620	6
$\gamma^1$ Del .....	197963	Oct 11	80	6330	$\leq 25$

atmospheres. Second, calculating a spectral synthesis of the Be II line region which includes 20 spectral lines, convolving that synthesis with the appropriate rotational broadening, and matching the observed and calculated spectra through a differential technique described below. Third, comparing the Hyades spectra with stars of known Be abundance and with

each other through the "differential spectroscopy" method described below.

For the first approach the continuum was placed interactively through previously selected high points over the entire region of spectrum observed. We display the results of this procedure for all eight Hyades stars over the 10 Å region around the Be II doublet in Figure 1. (The spectra shown have been smoothed over 3 pixels.) Equivalent widths were measured for the feature at 3131 Å on both smoothed and unsmoothed spectra. Several measurements were made which covered a range from the maximum to the minimum that could be reasonably thought to be that feature. The error in the means of those multiple measures over the range in possibilities was typically  $\pm 7$  mÅ for the worst cases. Errors due to the continuum placement are difficult to estimate. The abundances calculated from the model atmosphere abundance program, RAI10 (for which we are indebted to M. Spite), for a range of temperatures and Be/H abundances are shown in Figure 2. These are for Kurucz (1979) models with  $\log g = 4.5$  and microturbulence parameters of 1.4, 1.3, and 1.1 km s<sup>-1</sup> for

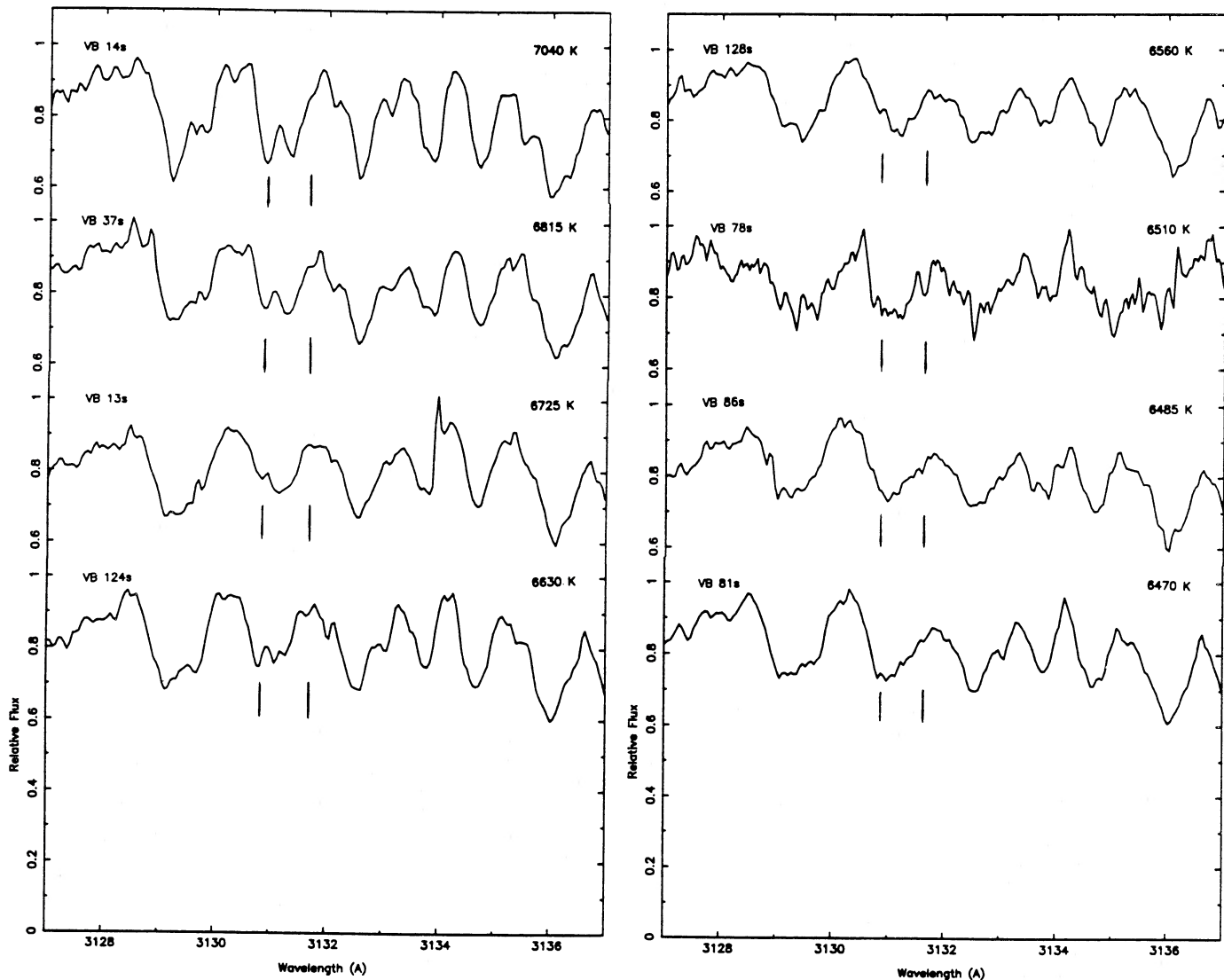


FIG. 1.—Spectra in the Be II region of stars in the Hyades cluster in order of decreasing temperature. The continua have been placed interactively with the aid of previously selected high portions. The positions of the two Be II lines are indicated. These spectra have been smoothed over three pixels.

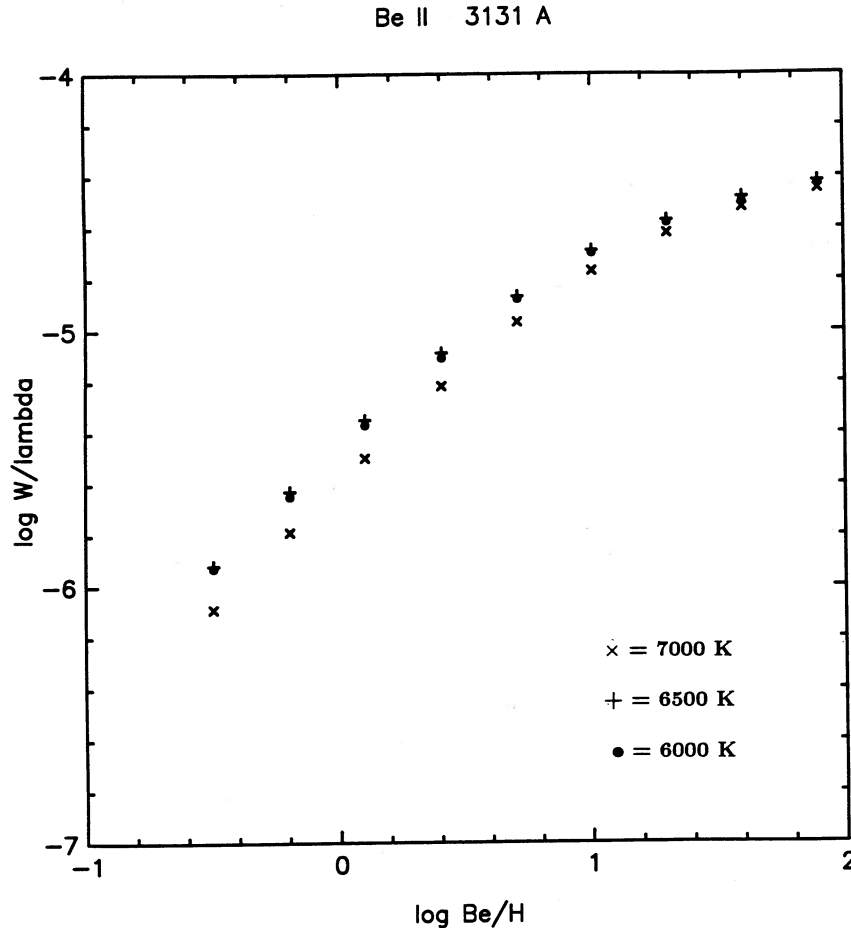


FIG. 2.—Calculated equivalent widths, expressed as  $\log(W/\lambda)$ , for the Be II line at  $\lambda 3131$  for given Be/H abundances with Kurucz (1979) model atmospheres for specific temperatures and  $\log g = 4.5$ . The microturbulence values were 1.4, 1.3, and 1.1  $\text{km s}^{-1}$  for  $T = 7000, 6500,$  and  $6000$  K, respectively. The curves for 6000 and 6500 K are virtually indistinguishable.

$T = 7000, 6500, 6000$  K, respectively, taken from Nissen (1981). There is very little dependence on temperature for the equivalent widths of the beryllium lines, understandably because this is a resonance transition of the dominant ionization stage. The equivalent widths and the Be/H abundances found in this way are given in § IV.

To solve the problems of uncertainty in the continuum position and the spectral blending (which is exacerbated by  $v \sin i$  values from 6 to 25  $\text{km s}^{-1}$ ), a “differential spectroscopy” procedure was used. This procedure included the following steps: First, a cross-correlation algorithm was used to match the wavelength scale of the object spectrum to a standard spectrum. The object spectrum was then multiplied by a low-order polynomial (usually linear) selected by a least-squares algorithm to give the best fit between the object and standard spectra in the region immediately around the Be doublet. Finally, the standard spectrum was subtracted from the object spectrum. The resulting difference spectrum shows any differences between the object and standard spectra; furthermore, if the continuum level is known for the standard, the equivalent width of the Be doublet can be obtained. This procedure was adapted to rapidly rotating stars by convolving the standard spectrum with a rotation profile of the correct width.

Figure 3 shows the results of this procedure as applied to the object star  $\iota$  Psc (heavy line at top) with the standard star

$\gamma^1$  Del (light line at top). The difference spectrum, showing the signature of Be, appears at the bottom of the figure. The temperatures of these two stars are 6190 K for  $\iota$  Psc and 6330 K for  $\gamma^1$  Del; that difference contributes little to the change in the profile appearance as there is virtually no change in the predicted Be line strengths between 6000 K and 6500 K as can be seen in Figure 2.

This procedure reduces the problems with close blends and, assuming the continuum level has been carefully determined for the standard stars, avoids the necessity of determining the continuum level for the object stars. However, it requires that standard stars of known Be abundance be available. We have selected Procyon ( $\alpha$  CMi, F5 IV–V) as our primary standard since we could get high S/N observation of it and because its temperature, 6620 K, is close to that of our Hyades stars. Although this star has spectral peculiarities and is located slightly above the main sequence, its spectrum shows no detectable Be. These peculiarities may result from the probable history of mass transfer between it and its white dwarf companion. Boesgaard (1976) found  $\text{Be}/\text{H} \leq 2.5 \times 10^{-13}$ . In addition, Procyon has a very small value of  $v \sin i$ . Our secondary standard was  $\gamma^1$  Del (F7V,  $T = 6330$ ), which also has a small value of  $v \sin i$ . It too is somewhat deficient in Be; see Figure 3.

The region around 3130 Å was synthesized by using the program RAI10 and the model atmospheres of Kurucz (1979).

## IOTA PSC VS. GAM-1 DEL

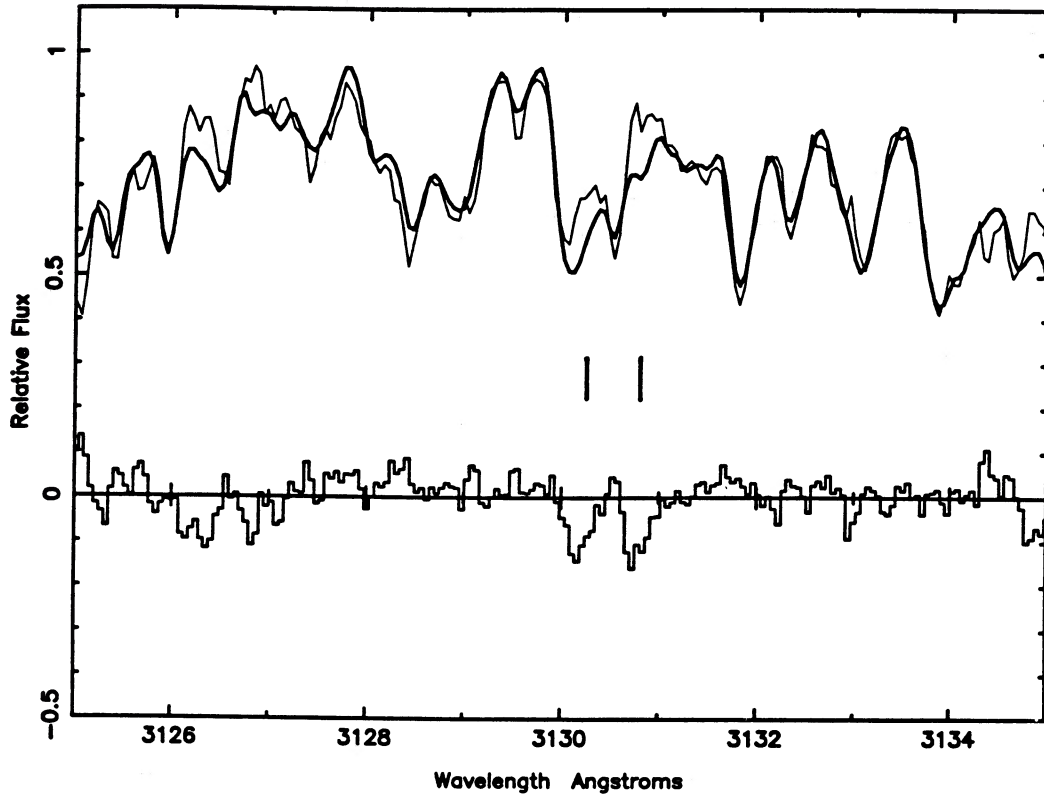


FIG. 3.—An example of the “differential” spectroscopy method (see text). The heavy line is the spectrum of  $\iota$  Psc, while the light line is that of the standard,  $\gamma^1$  Del. The difference spectrum is plotted below and shows the signature of Be II which is stronger in  $\iota$  Psc than in  $\gamma^1$  Del.

This program makes the usual assumptions of plane-parallel geometry and local thermodynamic equilibrium. The transitions considered in the synthesis are listed in Table 2 and are taken from Molaro and Beckman (1984). The abundances used for the elements other than Be are listed in Table 3 (Allen 1973). Although we have not included some of the more

unusual species with transitions in this region, we have included all of the more important transitions, and a comparison of the synthetic spectrum with the observed spectrum shows reasonable agreement. We did not attempt to derive astrophysical  $f$ -values or to modify the abundance values used in order to achieve better fits for the lines that blend with Be.

The spectral synthesis was carried out over a grid of three values of the temperature (6000 K, 6500 K, and 7000 K) and three values of the beryllium abundance [ $\log N(\text{Be})$  of 0.0, 0.5, and 1.0 on a scale of  $\log N(\text{H}) = 12$ ]. The abundances of the other elements included in the synthesis were held constant, as were the surface gravity at a value of  $\log g = 4.0$  and the microturbulence parameter at a value of  $1.5 \text{ km s}^{-1}$ . The synthesized spectra were, in addition, numerically convolved with a rotational profile appropriate for values of  $v \sin i$  of 10, 20, and  $40 \text{ km s}^{-1}$ . Figures 4 and 5 show the spectral synthesis for

TABLE 2  
LINES USED IN SPECTRAL SYNTHESIS

Wavelength (Å)	Ion	Excitation (eV)	$\log gf$
3129.30.....	Ni I	0.28	- 3.084
3129.34.....	Fe I	1.48	- 2.610
3129.76.....	Zr II	0.03	- 0.430
3129.93.....	Y II	3.39	0.640
3130.26.....	V II	0.35	- 0.277
3130.42.....	Be II	0.00	- 0.168
3130.54.....	Cr II	5.33	- 0.485
3130.79.....	Ti II	0.01	- 1.074
3131.07.....	Be II	0.00	- 0.468
3131.21.....	Cr I	3.11	- 0.001
3131.21.....	V I	1.22	- 0.423
3131.34.....	Fe II	3.81	- 3.553
3131.54.....	Cr II	4.18	- 1.283
3131.54.....	Cr II	4.17	- 1.545
3131.70.....	Ni I	3.31	- 2.164
3131.70.....	Ni I	3.31	- 1.272
3131.72.....	Fe II	4.08	- 1.855
3132.04.....	Cr II	2.48	0.454
3132.07.....	Zr I	0.54	0.020
3132.51.....	Fe I	3.21	- 0.924

TABLE 3  
ABUNDANCES USED IN SPECTRAL SYNTHESIS

Element	Log Abundance [ $\log N(\text{H}) = 12.0$ ]
Cr .....	5.50
Fe .....	7.65
Ni .....	6.40
Ti .....	5.50
V .....	3.90
Y .....	2.80
Zr .....	2.00

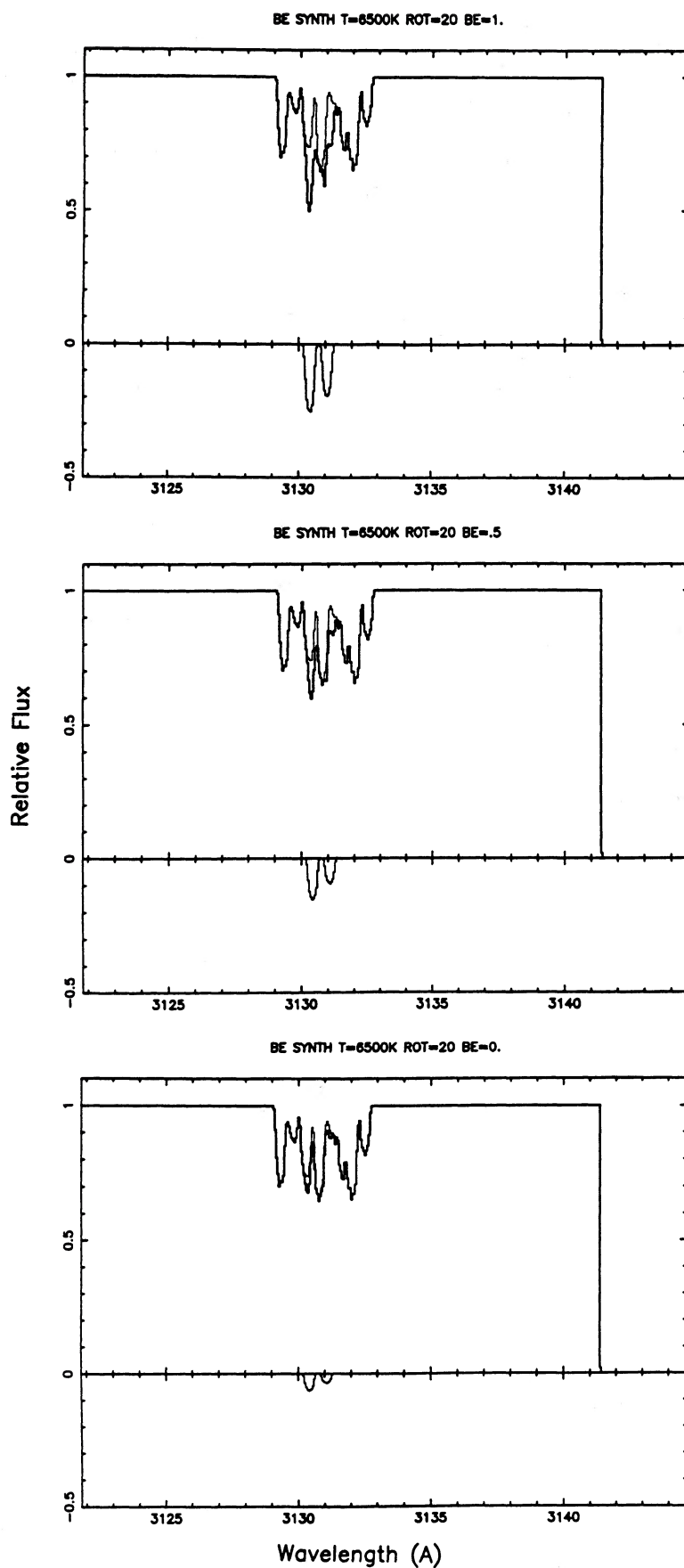
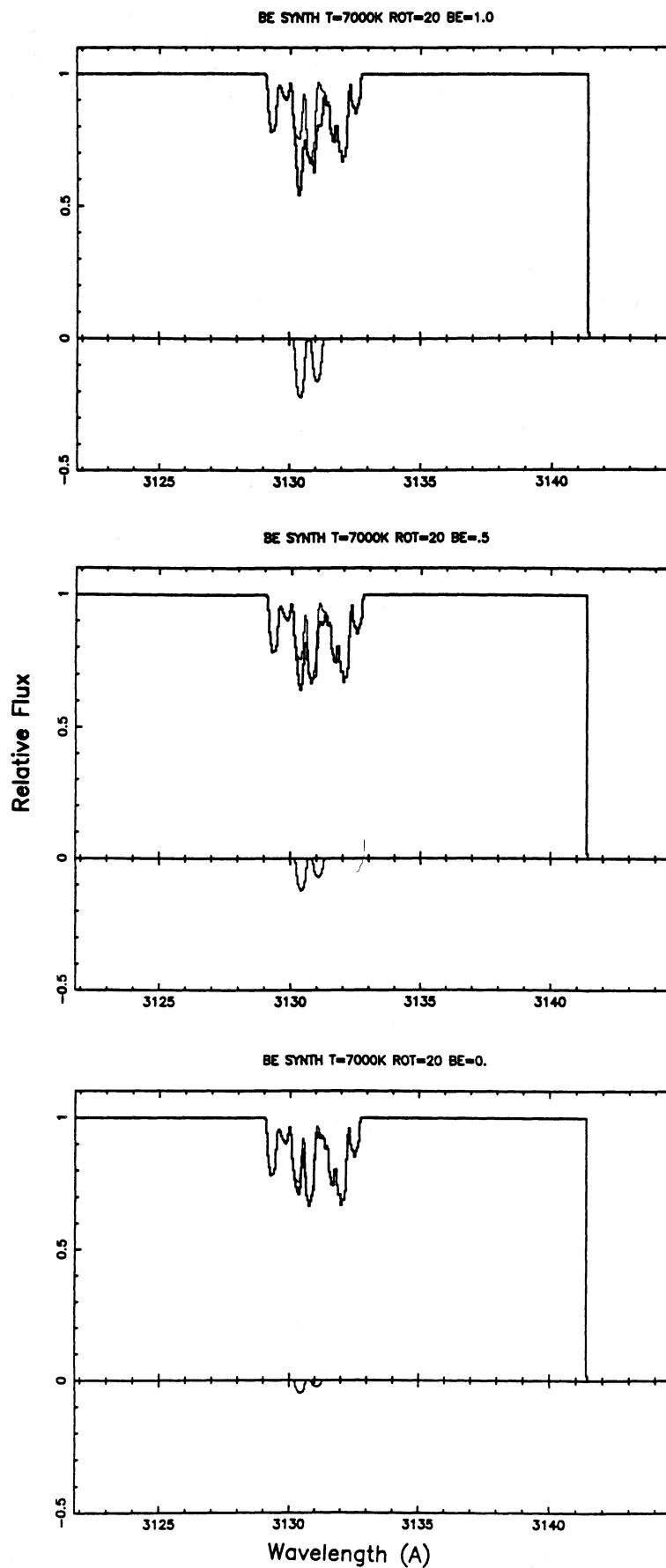


FIG. 4.—A series of spectral-synthesis profiles in the Be II region for  $T = 6500$  K and three Be/H abundances:  $\log N(\text{Be}) = 1.0, 0.5,$  and  $0.0$  (top to bottom) corresponding to  $\text{Be}/\text{H} = 10^{-11}, 3.2 \times 10^{-12},$  and  $10^{-12}$ . The synthetic spectra have been convolved with a rotational velocity profile corresponding to  $20 \text{ km s}^{-1}$ . Each panel also shows a light line corresponding to the synthesis with no Be II lines present. The difference spectrum between the given Be/H value and no Be is shown in the lower part of each panel.

FIG. 5.—Same as Fig. 4 except for  $T = 7000$  K

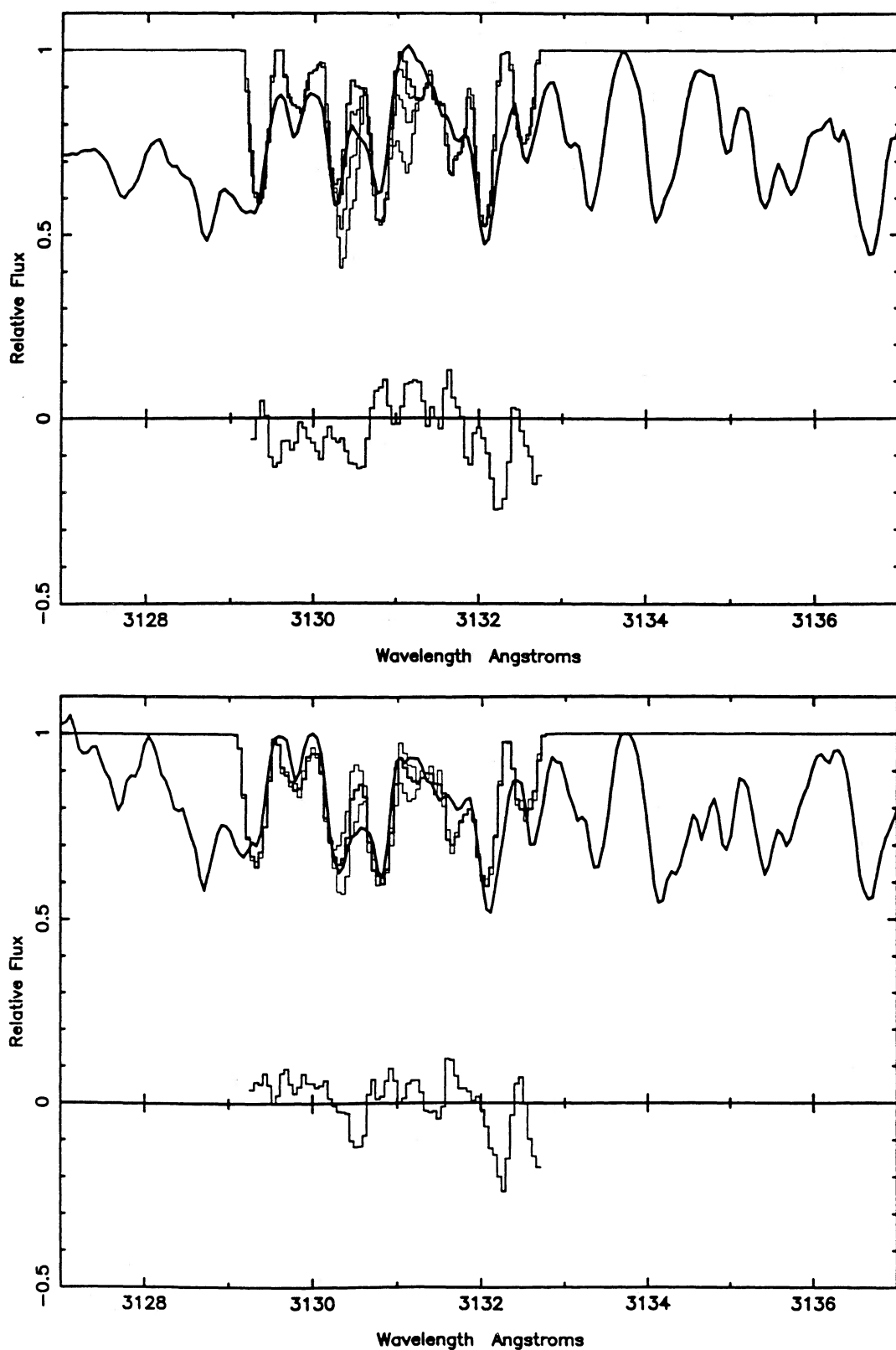


FIG. 6.—The observed (*heavy line*) and synthetic (*histogram-style lines*) spectra of  $\alpha$  CMi (*upper panel*) and  $\gamma^1$  Del (*lower panel*). The darkest line of the histogram synthesis corresponds to our best fit for the Be/H abundance and is the one used to form the difference spectrum shown in the lower part of the panels. For  $\alpha$  CMi the best fit is the one with no Be; the others shown have increasing amounts of Be/H:  $10^{-12}$ ,  $3 \times 10^{-12}$ , and  $10^{-11}$ . For  $\gamma^1$  Del the best fit is  $3 \times 10^{-12}$ ; the others shown are for  $10^{-12}$  and  $10^{-11}$ .

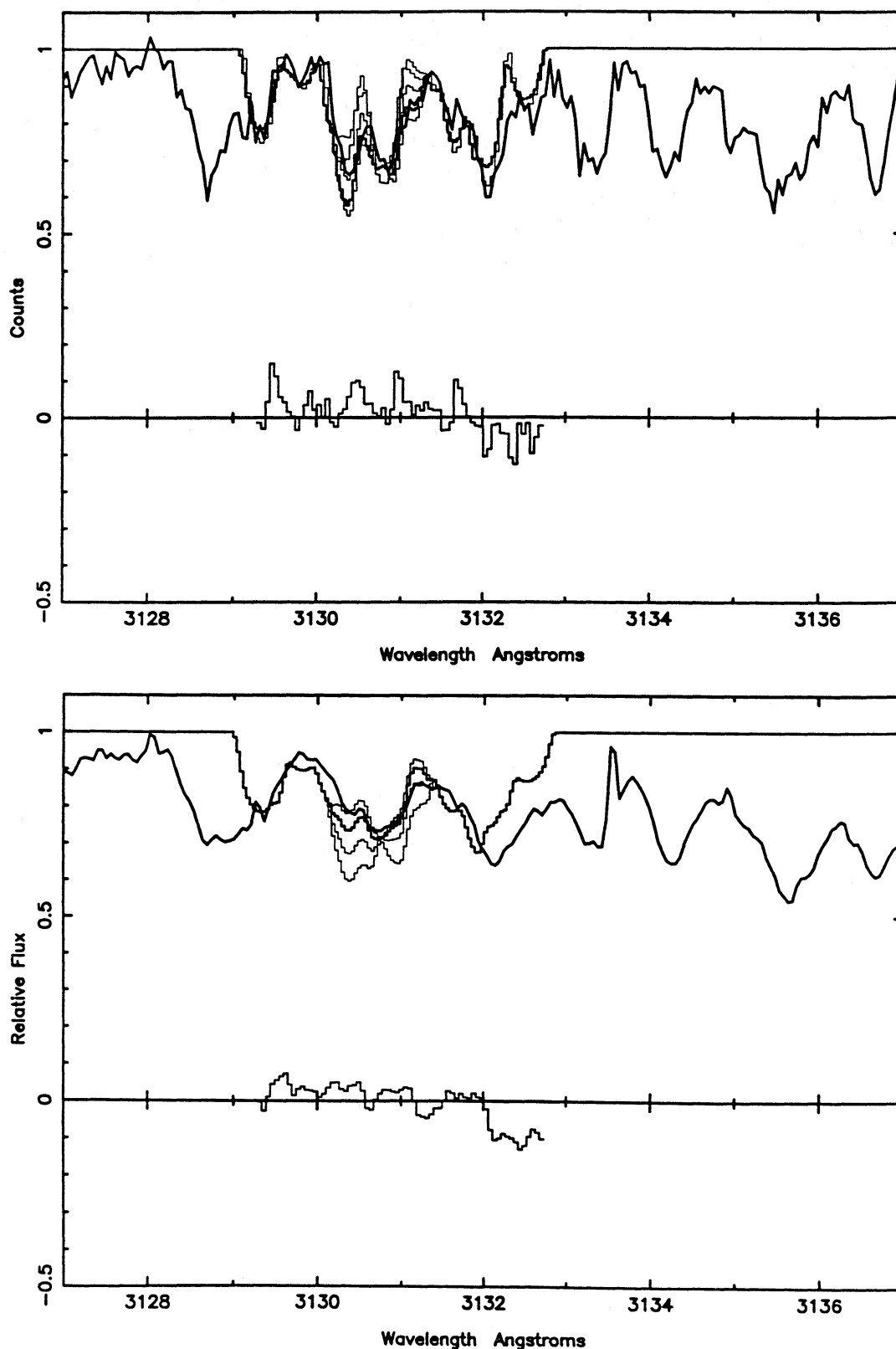


FIG. 7.—The same as Fig. 6 except the spectra are of VB 14 (*upper panel*) and VB 13 (*lower panel*). The darkest line of the histogram synthesis corresponds to our best fit for the Be/H abundance and is the one used to form the difference spectrum shown in the lower part of the panels. For VB 14 the best fit has  $7 \times 10^{-12}$ ; the others shown have values of Be/H of zero Be,  $10^{-12}$ ,  $3 \times 10^{-12}$ , and  $10^{-11}$ . For VB 13 there is no good fit, but the best fit is  $3 \times 10^{-12}$ ; the other shown are for zero Be,  $10^{-12}$  (*darkest histogram*), and  $10^{-11}$ . We tended to rely more on the fit with  $\lambda 3131$  than with the more blended line at  $\lambda 3130$ .

6500 K and 7000 K and the three values of  $\log N(\text{Be})$  and rotation of  $20 \text{ km s}^{-1}$ . In each case the upper plot shows the profiles with Be II lines at the abundance level given and the profiles without Be II lines; the lower plot shows the difference with and without Be. These plots can be directly compared with the series of observed spectra and difference spectra.

We have used our differential spectroscopy technique to match the synthetic spectra to the stellar spectra after having artificially rotationally broadened the synthetic spectrum to match the stellar spectrum. The results of this procedure are shown in Figures 6 and 7 for the standards  $\alpha$  CMi and  $\gamma^1$  Del and the Hyades stars VB 14 and 13. The observed spectrum is the solid dark line, while the calculated spectra are histogram-style with the best match as a darker histogram. The difference spectrum below is that between the observed and the best fit. It was not possible to match both Be II lines well, presumably due to the atomic and abundance values used for the blending lines. (A more convincing match, especially for  $\alpha$  CMi which is

known to have nonsolar abundances, could have been obtained by adjusting abundances and  $gf$ -values. That seemed to be more ad hoc and to consume more computer effort than we felt was warranted.) We tended to prefer to match the Be II line at  $3131 \text{ \AA}$ . The best match for  $\alpha$  CMi had no Be at all and that for  $\gamma^1$  Del was  $\text{Be}/\text{H} = 3 \times 10^{-12}$ , down an order of magnitude from the solar value (Chmielewski, Müller, and Brault 1975). For VB 14 the best fit appears to be  $\sim 7 \times 10^{-12}$ ; there is no good fit for the more rapidly rotating VB 13, but  $\sim 3 \times 10^{-12}$  appears to be the best.

The Hyades stars are all rotating more rapidly than either of the standards. As mentioned above, we convolved the standard star with a rotation profile of the appropriate width. We have made plots of all the Hyades stars with both "rotated" standards. Those plots with respect to  $\alpha$  CMi are shown in Figure 8; the plot for VB 78 is shown relative to  $\gamma^1$  Del because those two spectra were taken on the same observing run at a different dispersion from the others. The Hyades stars all clearly have

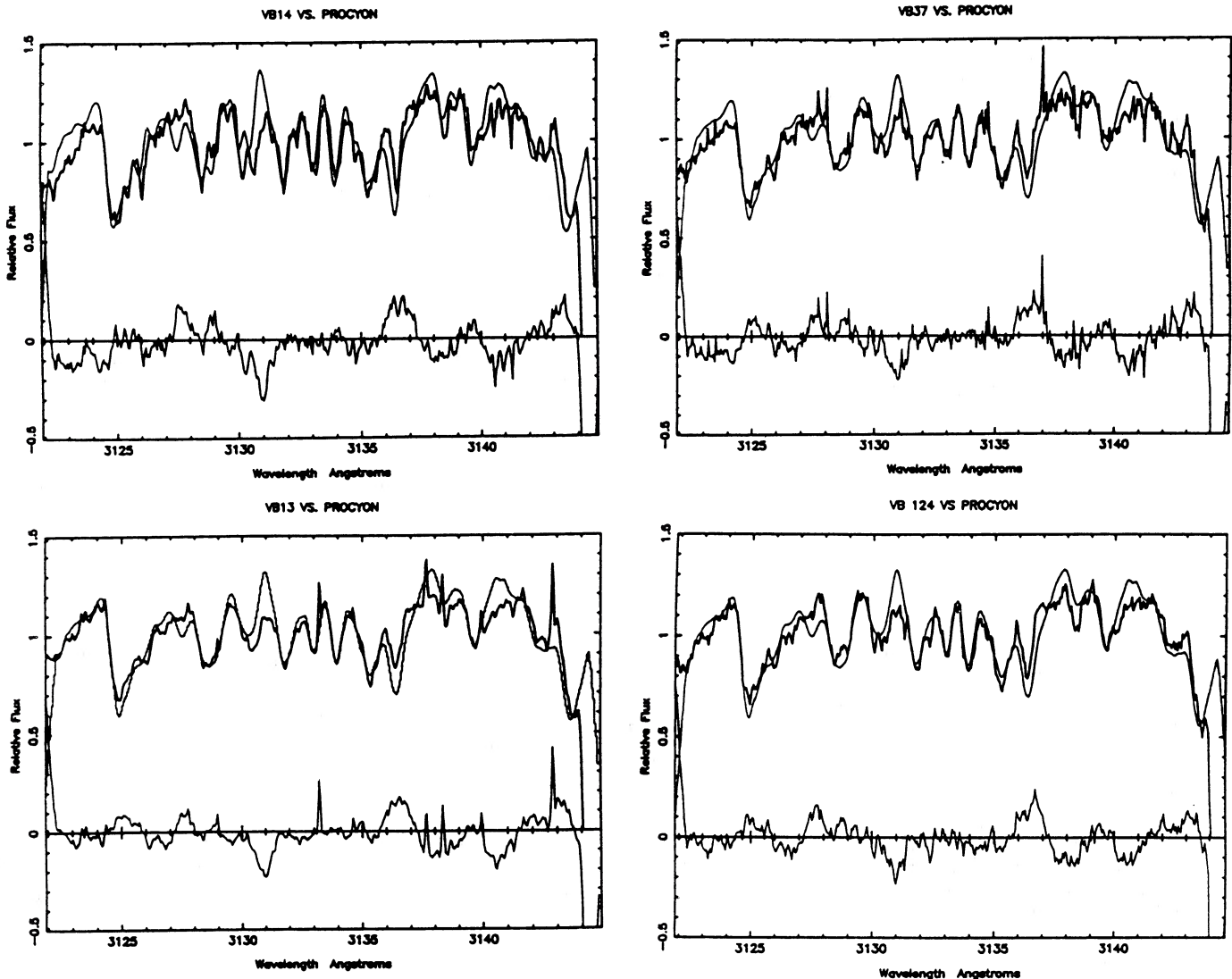


FIG. 8.—A montage of the Be II region spectra for the differential comparisons between each Hyades star (*heavy line*) with  $\alpha$  CMi (*light line*). (The spectrum of VB 78 is shown with that of  $\gamma^1$  Del since they were taken on the same night with the other grating.) In each case the Be II lines are clearly stronger in the Hyades stars and the Be signature can also be seen in the difference spectra. Due to the known spectral peculiarities of  $\alpha$  CMi, the spectra disagree in some other features too, but note the good agreement between VB 78 and  $\gamma^1$  Del.

more Be than  $\alpha$  CMi, and the features at 3131 Å is enhanced with a respect to  $\gamma^1$  Del. Because  $\alpha$  CMi does not match the Hyades stars exactly, notice in particular the regions near 3136 and 3140 Å, we show in addition some intercomparisons of the Hyades with each other. In order to determine empirically if there is any change in Be content through the Li gap, we have selected VB 13 as a Hyades "standard." VB 13 is in the middle of our temperature range with  $T = 6725$  K; it has a fairly typical  $v \sin i$  at  $18 \text{ km s}^{-1}$ , and its Li abundance is the lowest of the stars we were able to observe for Be with  $\log N(\text{Li}) \leq 1.54$  (Boesgaard and Tripicco 1986). Figure 9 shows that series of comparisons. From this it appears that all Hyades stars have about the same Be content as VB 13, with the possible exception of the hottest stars, VB 14, which seems to have more Be than VB 13. This is clear from this straightforward comparison of the observations even though we are not content with our spectrum synthesis fit to VB 13; i.e., there is no significant dip corresponding to the Li dip.

## IV. RESULTS

The abundance results are presented in Table 4. The Be abundances are plotted, along with the Li abundances, with respect to temperature in Figure 10. It is clear that there is no dramatic drop in Be in the temperature region  $T = 6500$ – $6800$  K as there is in the Li abundance. This is not particularly surprising when one considers that Be is destroyed at temperatures of  $\sim 3.5 \times 10^6$  K while Li is destroyed at only  $\sim 2.5 \times 10^6$  K. We cannot rule out a drop of a factor of 2–4 across the Li gap and it does appear that VB 14, the hottest star, has more Be than the others. We note that Boesgaard, Heacox, and Conti (1977) also observed VB 14 and VB 37 and found virtually the same values of Be/H as determined here, viz.  $1.1 \times 10^{-11}$  and  $8.5 \times 10^{-12}$ , respectively.

Although there is no evidence for Be deficiencies, the presence of so many blending lines and the relatively rapid rotation of these stars make the absolute values of Be/H uncertain.

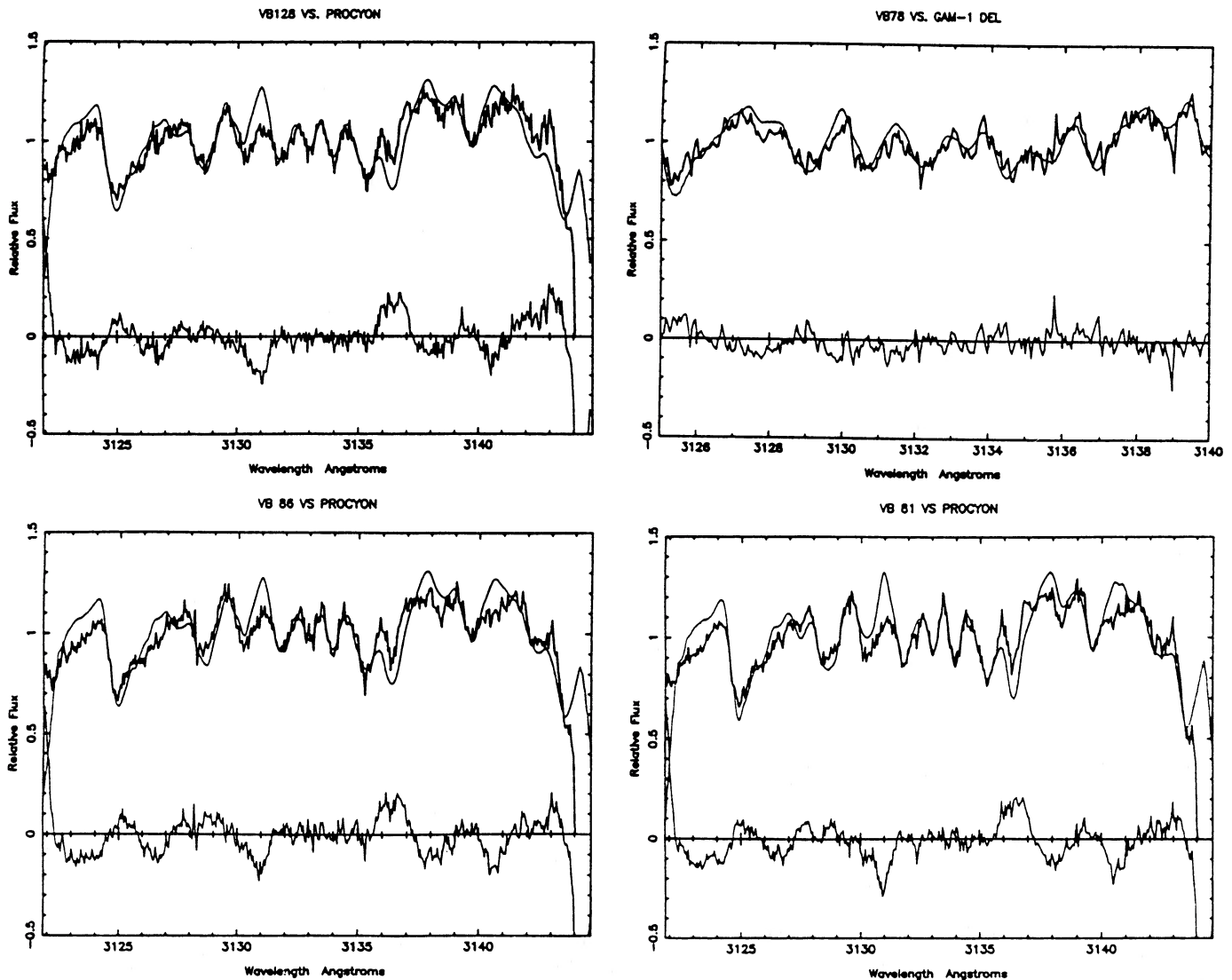


FIG. 8—continued

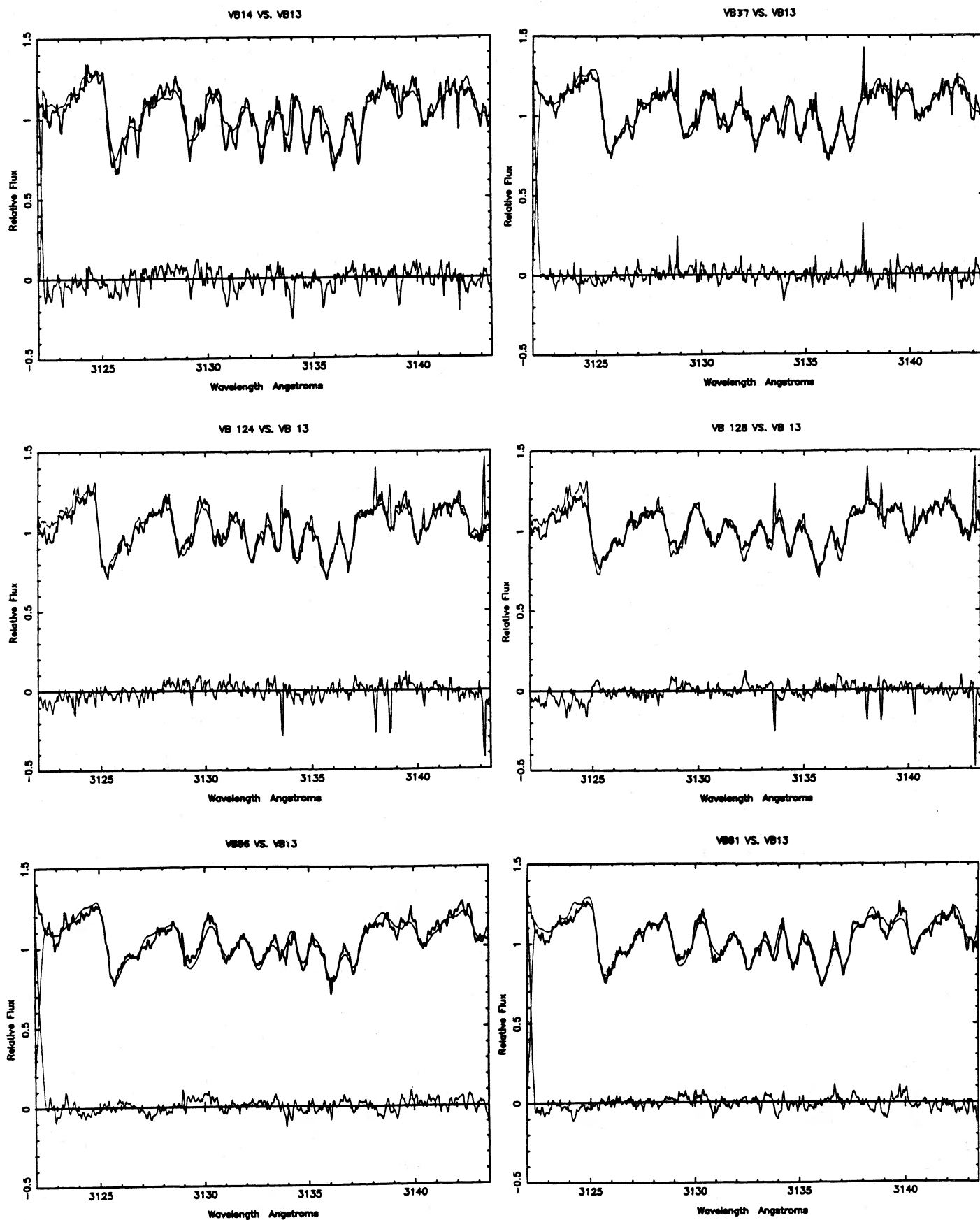


FIG. 9.—A montage of the Be II region showing the comparisons of other Hyades stars with VB 13. It appears that VB 14 has more Be than VB 13; however, the other stars, going across the Li gap in temperature, have the same amount of Be as VB 13. (The sharp spikes are due to incomplete removal of the cosmic-ray events.)

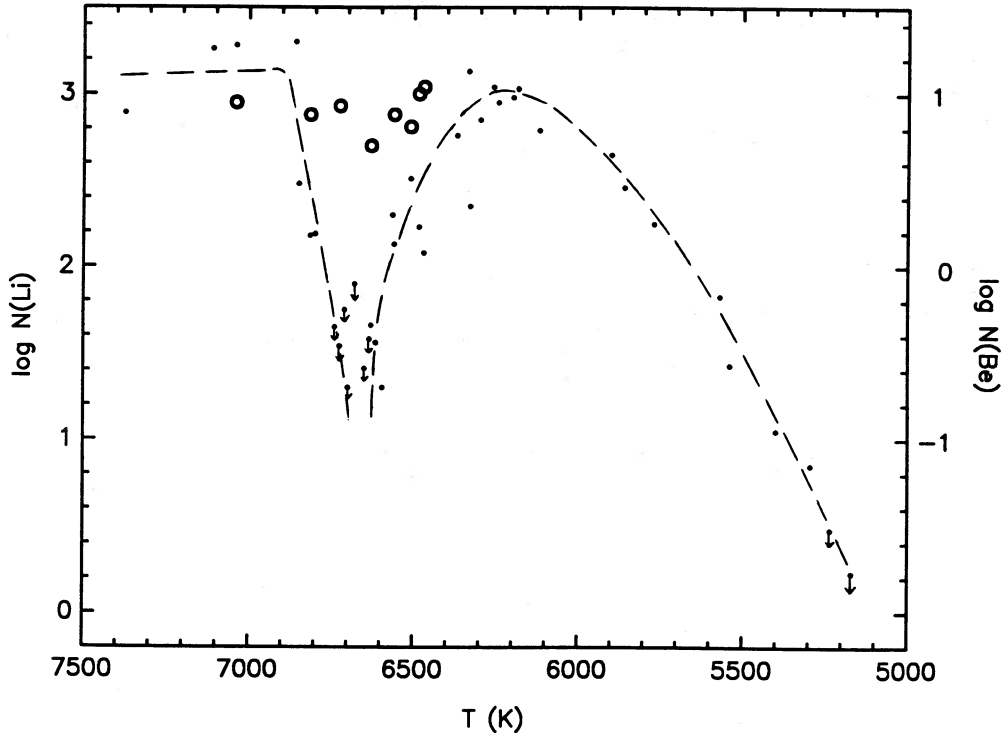


FIG. 10.—Lithium abundances [on the scale where  $\log N(\text{H}) = 12.00$ ] (small dots) and Be abundances (open circles) plotted against temperature for the Hyades cluster. The arrows represent upper limits. The Li results are from Boesgaard and Tripicco (1986), Boesgaard and Budge (1988), and for the cooler stars from Cayrel *et al.* (1984). The dashed line represents the Li-temperature profile for the Hyades. There is little or no Be depletion across the temperature interval where Li is severely depleted.

We have used three techniques to find the abundances: curves of growth, spectral synthesis, and differential spectroscopy. Each method contains its own uncertainties. For the first method errors in the temperature play no role but those in the equivalent width measurement of  $\sim 7 \text{ m\AA}$  or  $\sim 13\%$  results in Be/H errors of about  $\pm 25\%$ . For the second method Figures 6 and 7 show what differences a factor of 3 in Be abundances

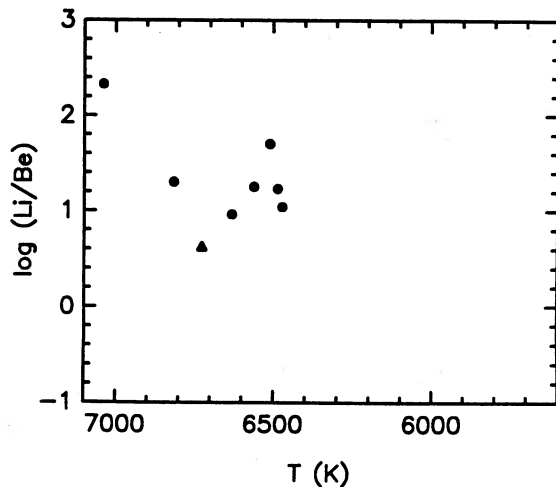


FIG. 11.—Lithium/beryllium abundance ratios vs. temperature for the Hyades stars. This is the counterpart to Fig. 13 of Charbonneau and Michaud given for comparison with their predictions. The Li/Be ratio apparently does not provide a strong test of their theory but all values found here are consistent.

does to the line profile. For our signal-to-noise (about 100 per pixel) and 3 pixel smoothing, the fits are better than a factor of 2 for the 3131 Å line. The first and second method agree in the average ratio by a factor of 1.8. The differential method reduces the difficulties with the continuum placement. We estimate that Be/H could be in error by as much as a factor of 2. We know the relative values of Be/H well, however, and across this temperature range these stars all have approximately the same Be/H.

The Li gap in the Hyades has been explained as a consequence of diffusion (gravitational settling) by Michaud (1986), of meridional circulation by Charbonneau and Michaud (1988), and of turbulent mixing induced by rotation by Vauclair (1988). Charbonneau and Michaud (1988) have also made predictions about the Li/Be ratio from their model. In Figure 11 we plot the counterpart of their Figure 13 of the Li/Be ratio. It seems that this does not represent a critical test for their theory as all the values are in the acceptable range. Calculations on the effects of diffusion on Be and of turbulent mixing on Be may help to understand what hydrodynamic mixing processes best explain the combined results for Li and Be in the Hyades.

We are very grateful for the skillful help at the telescope of John Varsik. This work was started while A. M. B. was a Guggenheim Fellow and then a Visiting Professor at Caltech; that support and the hospitality at Caltech are greatly appreciated. This work was supported by NSF grants AST-8216192 and RII-8521715 to A. M. B. and by an NSF Graduate Fellowship to K. G. B.

TABLE 4  
ABUNDANCES RESULTS

VB	T (K)	$W_{3131}$ (mÅ)	Be/H <sup>a</sup>	Be/H <sup>b</sup>	log N(Li)	log Li/Be <sup>c</sup>
14 .....	7040	48	$9 \times 10^{-12}$	$7 \times 10^{-12}$	3.28	2.3
37 .....	6815	47	$7.5 \times 10^{-12}$	$3 \times 10^{-12}$	2.18	1.3
13 .....	6725	53	$8.5 \times 10^{-12}$	$3 \times 10^{-12}$	$\leq 1.54$	$\leq 0.6$
124 .....	6630	39	$5 \times 10^{-12}$	$3 \times 10^{-12}$	1.66	1.0
128 .....	6560	52	$7.5 \times 10^{-12}$	$3 \times 10^{-12}$	2.13	1.2
78 .....	6510	48	$6.5 \times 10^{-12}$	$7 \times 10^{-12}$	2.51	1.7
86 .....	6485	65	$1 \times 10^{-11}$	$7 \times 10^{-12}$	2.23	1.2
81 .....	6470	66	$1.1 \times 10^{-11}$	$7 \times 10^{-12}$	2.08	1.0

<sup>a</sup> From Be II  $\lambda 3131$  and curve of growth.

<sup>b</sup> From synthesis or comparison with  $\gamma^1$  Del and  $\alpha$  CMi.

<sup>c</sup> With Be/H from *a*.

## REFERENCES

- Allen C. W. 1973, *Astrophysical Quantities* (3d ed; London: Athlone).  
 Boesgaard, A. M. 1976, *Ap. J.*, **210**, 466.  
 Boesgaard, A. M., and Budge, K. G. 1988, *Ap. J.*, **332**, in press.  
 Boesgaard, A. M., Heacox, W. D., and Conti, P. S. 1977, *Ap. J.*, **214**, 124.  
 Boesgaard, A. M., and Lavery, R. J. 1986, *Ap. J.*, **309**, 762.  
 Boesgaard, A. M., and Tripicco, M. J. 1986, *Ap. J. (Letters)*, **302**, L49.  
 Budge, K. G., Boesgaard, A. M., and Varsik, J. 1988, In *IAU Symposium 132, The Impact of Very High S/N Spectroscopy on Stellar Physics*, (Dordrecht: Kluwer), p. 577.  
 Cayrel, R., Cayrel de Strobel, G., Campbell, B., and Däppen, W. 1984, *Ap. J.*, **283**, 205.  
 Charbonneau, P., and Michaud, G. 1988, *Ap. J.*, **334**, 746.  
 Chmielewski, Y., Müller, E. A., and Brault, J. W. 1975, *Astr. Ap.*, **42**, 37.  
 Kurucz, R. L. 1979, *Ap. J. Suppl.*, **40**, 1.  
 Michaud, G. 1986, *Ap. J.*, **302**, 650.  
 Molaro, P., and Beckman, J. 1984, *Astr. Ap.*, **139**, 394.  
 Nissen, P. 1981, *Astr. Ap.*, **97**, 145.  
 Vauclair, S. 1988, *Ap. J.*, **335**, 971.

ANN MERCHANT BOESGAARD: Institute for Astronomy, 2680 Woodlawn Drive, Honolulu, HI 96822

KENT G. BUDGE: Astronomy Department, 105-24, California Institute of Technology, Pasadena, CA 91125